

## Spatial manipulation of magnetic damping in ferromagnetic-antiferromagnetic films by ion irradiation

Jeffrey McCord,<sup>1,\*</sup> Thomas Strache,<sup>1</sup> Ingolf Mönch,<sup>2</sup> Roland Mattheis,<sup>3</sup> and Jürgen Fassbender<sup>1</sup>

<sup>1</sup>*Helmholtz-Zentrum Dresden Rossendorf e.V., P.O. Box 510119, D-01314 Dresden, Germany*

<sup>2</sup>*Leibniz Institute for Solid State and Materials Research IFW Dresden, P.O. Box 270116, D-01171 Dresden, Germany*

<sup>3</sup>*IPHT Jena, Albert-Einstein-Straße 9, D-07745 Jena, Germany*

(Received 22 February 2011; published 20 June 2011)

The spatial manipulation of the effective magnetic damping parameter in ferromagnetic-antiferromagnetic-ferromagnetic film systems is shown. By applying ultrathin antiferromagnetic layers in Ni<sub>81</sub>Fe<sub>19</sub>/IrMn/Ni<sub>81</sub>Fe<sub>19</sub> sandwich structures in combination with low fluence Ni-ion irradiation, a lateral control of the effective magnetic damping parameter is achieved. With irradiation, an interfacial intermixing and roughening is introduced, by which the interfacial coupling mechanisms and the magnetic state of the interlayer are altered. We find an exponential decay of all relevant magnetic property parameters with irradiation. Local irradiation is then applied to generate a magnetic layer with spatially distributed regions of different values of damping. The resulting overall relaxation time of the mixed property film is a direct superposition of the individual relaxation contributions. Thereby, the ratio of the phases with individual damping parameter determines the resulting overall damping.

DOI: [10.1103/PhysRevB.83.224407](https://doi.org/10.1103/PhysRevB.83.224407)

PACS number(s): 75.70.-i

### I. INTRODUCTION

The control of static and especially dynamic magnetic response of ferromagnetic (F) thin films is one of the biggest challenges in applied magnetism. Therefore, the adjustment of magnetic anisotropy and the connected resonance frequency, as well as the magnetic damping parameter, are of fundamental importance to ensure functionality in existing and envisioned spintronic applications.<sup>1-3</sup> One possibility to influence the magnetic properties of thin films is the modification of the bulk material's properties, such as changing the composition of the material.<sup>4</sup> Recently, it has been shown that by introducing rare-earth or transition metals, the magnetic damping parameter in F films can be altered in the ferromagnetic parent material.<sup>5-8</sup> Interfacial contributions in magnetic multilayers facilitate another path of spin engineering of magnetic thin-film properties. The most prominent example is the introduction of out-of-plane perpendicular anisotropy in magnetic multilayers.<sup>9</sup> For such systems, it has been shown that the magnetic anisotropy can be converted from out-of-plane to in-plane in character by ion-irradiation-induced interfacial mixing, hence creating a magnetic property patterning.<sup>10</sup> Moreover, a transition from antiferromagnetic to ferromagnetic coupling by local ion irradiation has been achieved in exchange-coupled sandwich structures.<sup>11</sup> Another relevant area of interface magnetism is the creation of a unidirectional anisotropy or exchange bias with the use of antiferromagnetic (AF) materials in thin-film multilayers,<sup>12-15</sup> by which also a congruent increase of precessional frequency and magnetic damping is initiated.<sup>16-19</sup> The origin of the AF layer-induced enhancement of damping is due to a combination of two-magnon scattering and additional interfacial magnetic dispersion effects.<sup>16,20</sup> For very thin AF layer thickness, below or around the onset of exchange bias, a local spin fluctuation based contribution to damping from quasi-superparamagnetic AF grains is discussed.<sup>21</sup> In this paper, we demonstrate the spatial and exclusive tailoring of magnetic damping effects in F-AF-F sandwich structures by ion irradiation. The modification is achieved with a minimal influence on other magnetic properties.

### II. SAMPLE PREPARATION

A series of Si-SiO<sub>2</sub>-Ta(4 nm)-Ni<sub>81</sub>Fe<sub>19</sub> (15 nm)-Ir<sub>23</sub>Mn<sub>77</sub>-Ni<sub>81</sub>Fe<sub>19</sub> (15 nm) sandwich structures with varying AF layer thickness  $t_{\text{IrMn}} = 0-2.50$  nm were prepared by dc-magnetron sputtering in a multitarget ultrahigh-vacuum sputter system with a base pressure below  $23 \times 10^{-8}$  Torr at an Ar pressure of  $53 \times 10^{-3}$  Torr. To induce a uniaxial magnetic anisotropy, a magnetic field  $H_{\text{dep}} = 100$  Oe was applied during film deposition. No protection layers were used to avoid secondary intermixing effects during ion irradiation. Therefore, for the given sandwich structure, only Ni<sub>81</sub>Fe<sub>19</sub> to IrMn interfaces are relevant. No post-annealing steps, which potentially would induce additional mixing at the interface, were performed.

### III. EXPERIMENTS AND DISCUSSION

The quasistatic reversal characteristics were deduced from inductive magnetometry. The exchange-bias field  $H_{\text{eb}}$  was obtained from the magnetization loop shift along the magnetically easy axis parallel to  $H_{\text{dep}}$ . The variation of coercivity  $H_c$  and field  $H_{\text{eb}}$  with  $t_{\text{IrMn}}$  is displayed in Fig. 1. For  $t_{\text{IrMn}} \leq 2.50$  nm, no exchange bias is observed, only  $H_c$  increases sharply around  $t_{\text{IrMn}} = 2.25$  nm. Below that thickness, only a minor increase of  $H_c$  with  $t_{\text{IrMn}}$  is found (see also the inset of Fig. 1). This behavior is in agreement with the results obtained from regular bilayer F/AF systems.<sup>17,22</sup> Effects from different coupling strengths<sup>23</sup> from the top (F/AF) or bottom (AF/F) AF interface are not observed below the onset of exchange bias.

The corresponding dynamic magnetic properties of the films were characterized by pulsed inductive microwave magnetometry (PIMM),<sup>24</sup> whereby the precessional frequency  $f_{\text{res}}$  and the effective magnetic damping parameter  $\alpha_{\text{eff}}$  and relaxation time  $\tau_{\text{rel}}$ , respectively, were derived from analysis of the damped oscillation of the measurement signal.<sup>25</sup> All measurements were performed with an applied magnetic field  $H_{\text{bias}}$  to ensure a single magnetic domain state. Exemplary measurement data for different  $t_{\text{IrMn}}$  are shown in Fig. 2(a). Comparing Fig. 1(d) to Fig. 2(d), the AF-induced increase of

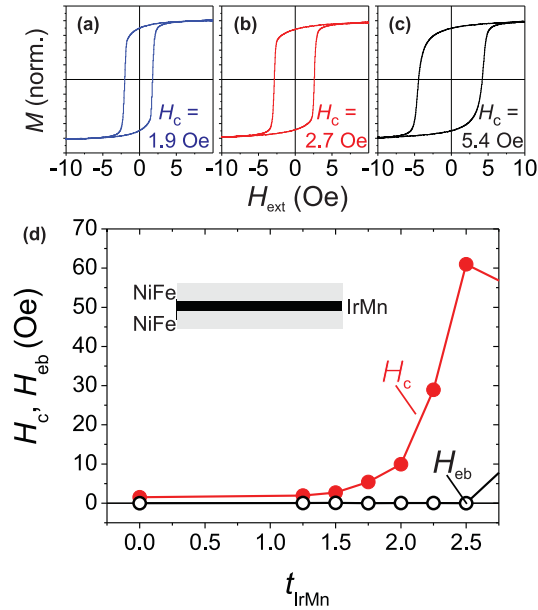


FIG. 1. (Color online) (a)–(c) Magnetization loops obtained from  $\text{Ni}_{81}\text{Fe}_{19}$  (15 nm)-IrMn ( $t_{\text{IrMn}}$ )- $\text{Ni}_{81}\text{Fe}_{19}$  (15 nm) trilayers with different AF layer thickness  $t_{\text{IrMn}} = 1.25, 1.50$ , and  $1.75$  nm. The respective coercive fields  $H_c$  are indicated. (d) Change of  $H_c$  and exchange bias field  $H_{\text{eb}}$  with  $t_{\text{IrMn}}$ . The principal structure of the layer stack is indicated.

$f_{\text{res}}$  starts at  $t_{\text{IrMn}} = 1.75$  nm, which is well below the appearance of exchange bias. Moreover,  $\alpha_{\text{eff}}$  sets in at even lower values of AF thickness, almost doubling at  $t_{\text{IrMn}} = 1.50$  nm and then drastically increasing up to a value of  $\alpha_{\text{eff}} = 0.055$  for  $t_{\text{IrMn}} = 1.75$  nm. Overall, a major change of static and

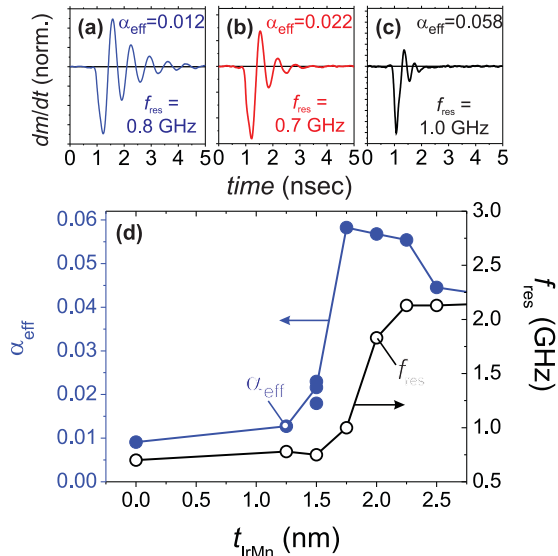


FIG. 2. (Color online) (a)–(c) Dynamic magnetic response  $dm/dt$  to a rf-magnetic pulse field<sup>24</sup> in  $\text{Ni}_{81}\text{Fe}_{19}$  (15 nm)-IrMn- $\text{Ni}_{81}\text{Fe}_{19}$  (15 nm) structures for  $t_{\text{IrMn}} = 1.25, 1.50$ , and  $1.75$  nm. A magnetic bias field  $H_{\text{bias}} = 30$  Oe is applied during the measurements. The values of zero-field precessional frequency  $f_{\text{res}}$  and effective magnetic damping parameter  $\alpha_{\text{eff}}$  are indicated. (d) Variation of  $f_{\text{res}}$  and  $\alpha_{\text{eff}}$  with AF layer thickness  $t_{\text{IrMn}}$ .

dynamic magnetic properties is achieved by varying  $t_{\text{IrMn}}$  by only 1.0 nm. However, within this small range of AF layer thickness, the onset of magnetic property change is different for the individual magnetic property parameters. As will be shown next, the incremental onset of magnetic property alteration facilitates the almost exclusive adjustment of  $\alpha_{\text{eff}}$ .

For that reason, a sandwich with  $t_{\text{IrMn}} = 1.5$  nm was irradiated with Ni ions of different fluence. Ni as an element was chosen, as it is the main component of the F film in the sandwich structure and therefore only minor compositional changes in the F material are obtained with ion irradiation. The irradiation of the sandwich has two main effects: It introduces roughness at the F-AF interface and it also changes in the material composition around and within the AF layer. To distinguish between both effects, the process of ion irradiation was simulated using the TRIM code of the SRIM package.<sup>26</sup> The calculated depth distributions of damage, i.e., the number of target displacements, being the sum of generated vacancies and replacement collisions, of layer atoms per incoming ion is displayed in Fig. 3(a). An irradiation energy of 40 keV was chosen to ensure that the ion-induced damage distribution would be situated within the magnetic layers and would not reach the bottom F-substrate interface. From these results, the mean damage at the AF layer can be

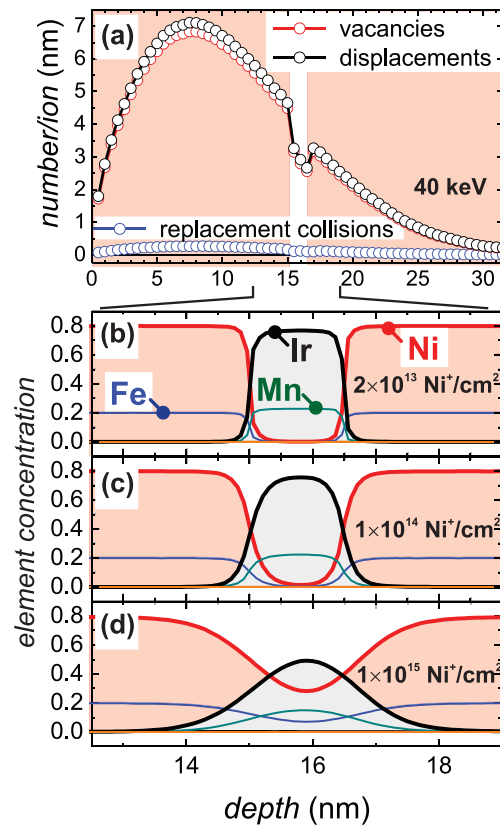


FIG. 3. (Color online) (a) TRIM simulation results of the ion-irradiation impact events per ion with Ni-ion irradiation at 40 keV in  $\text{Ni}_{81}\text{Fe}_{19}$  (15 nm)/IrMn (1.50 nm)/ $\text{Ni}_{81}\text{Fe}_{19}$  (15 nm). The structure of the layer stack is indicated. (b)–(d) TRIDYN calculation results on interfacial mixing and alloying effects with different amounts of Ni-ion irradiation. The atomic concentrations are shown across the layer boundaries. The individual Ni-ion fluences are indicated.

estimated to approximately four displacements per target atom per  $10^{15}$  cm<sup>2</sup> incident Ni<sup>+</sup> ions. The compositional changes with increasing irradiation fluence were derived from Monte-Carlo-based binary collision computer simulations (TRIDYN<sup>27</sup>) using the same parameters as for the SRIM modeling. The profiles of the atomic species distributions in the center of the Ni<sub>81</sub>Fe<sub>19</sub>-Ir<sub>23</sub>Mn<sub>77</sub>-Ni<sub>81</sub>Fe<sub>19</sub> stack for different Ni-ion fluences are displayed in Figs. 3(b)–3(d). For low fluences, mainly the interface structure is altered due to interfacial intermixing. The interfaces become more rough. At larger fluences, alloying of the initially AF layer takes place, and a complete compositional alteration of the original IrMn composition is derived from the simulations. Even for the large Ni<sup>+</sup> fluence of  $10^{15}$  cm<sup>2</sup>, the maximum calculated percentage change of Ni concentration in the original Ni<sub>81</sub>Fe<sub>19</sub> film due to Ni implantation is 0.6%, and thereby no relevant modifications of magnetic properties other than from the intermixing effects are presumed to occur in the layer stack.

The effect of irradiation-induced intermixing at the F-AF interfaces on the static and dynamic magnetic properties is displayed in Fig. 4. The samples were irradiated at room temperature with Ni<sup>+</sup> ions with different fluences  $f(\text{Ni}^+)$ . An almost immediate decay of coercivity and damping with fluence is found. This indicates a strong connection between the initial interfacial modifications and the change in magnetic properties. The results are in accordance with irradiation-induced interfacial changes obtained in exchange-bias samples with much thicker AF layers<sup>28</sup> as well as with exchange-coupled multilayer films.<sup>29</sup> In contrast, ion-induced changes of characteristic magnetic bulk properties occur linearly with irradiation fluence.<sup>30,31</sup> As expected, no exchange-bias effect is initialized with irradiation. As demonstrated in Fig. 4(b), the

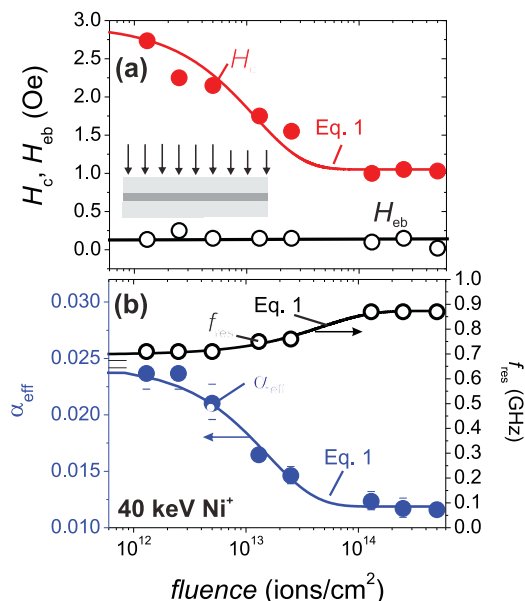


FIG. 4. (Color online) (a) Change of coercivity  $H_c$  and exchange bias field  $H_{\text{eb}}$  with fluence of Ni-ion irradiation in Ni<sub>81</sub>Fe<sub>19</sub> (15 nm)/IrMn (1.50 nm)/Ni<sub>81</sub>Fe<sub>19</sub> (15 nm). (b) Corresponding change of precessional frequency  $f_{\text{res}}$  and effective magnetic damping parameter  $\alpha_{\text{eff}}$ . Both graphs are plotted on a semilogarithmic scale.

original precession frequency  $f_{\text{res}}$  in the sandwich structures increases only by a small amount,  $\Delta f_{\text{res}} \approx 100$  MHz, with irradiation. Yet a strong decrease in  $\alpha_{\text{eff}}$  with increasing fluence is found, approaching a value close to the bulk Ni<sub>81</sub>Fe<sub>19</sub> damping parameter. For the given example,  $\alpha_{\text{eff}}$  reduces from 0.024 down to 0.011. The change of magnetic properties follows nearly an exponential decay law. The exact origin of this dependency is not clear, but an irradiation-induced increase of interfacial intermixing or roughness is expected to result in a strong and exponential decrease of exchange coupling between the FM and AF layers.<sup>28,32</sup> The lines in Fig. 4 are fits to the exponential dependency (Fig. (1)). Exemplarily, for  $\alpha_{\text{eff}}^{\text{irr}}$  we obtain

$$\alpha_{\text{eff}}^{\text{irr}} = \alpha_{\text{eff}}^{\infty} - C e^{-\frac{f(\text{Ni}^+)}{f_0}}, \quad (1)$$

where  $\alpha_{\text{eff}}^{\infty}$  is the saturation value of the damping parameter for strongly intermixed layers. The exponential decay rate  $f_0$  for all magnetic parameters is in the order of  $f_0 \approx 5 \times 10^{13}$  cm<sup>2</sup>. The sharp reduction of damping with irradiation also indicates an interfacial origin of increased damping in the F-AF-F structures. Above  $f(\text{Ni}^+) = 10^{14}$  cm<sup>2</sup>, the saturation value of magnetic damping  $\alpha_{\text{eff}}^{\infty}$  is nearly obtained.

The irradiation-induced change of damping now offers the opportunity to *laterally* change the effective damping parameter, as will be shown in the following. This is achieved by masking the film with a photolithographic mask and then selectively irradiating the magnetic layers, as sketched in Fig. 5(a). For the presented results, the film was masked with a wavelength of 10  $\mu\text{m}$ . By laterally varying the duty cycle of the square

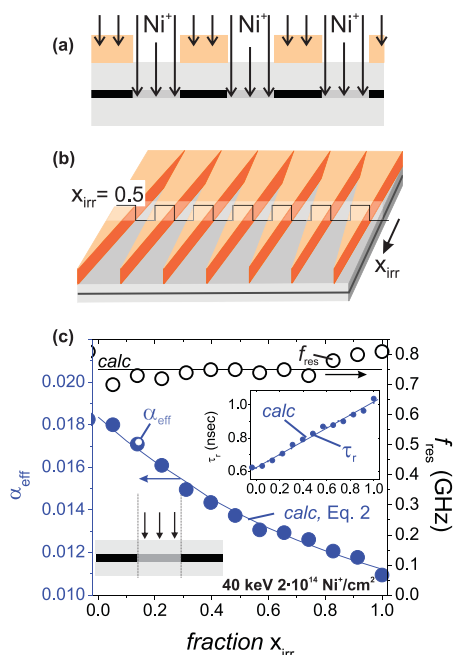


FIG. 5. (Color online) (a) Process of local irradiation through a stripelike photoresist mask. (b) Sample design for obtaining a sample with a gradient in the masked area. (c) Measured change of magnetic damping parameter  $\alpha_{\text{eff}}$  and precessional frequency  $f_{\text{res}}$  in dependence on the fraction  $x_{\text{irr}}$  of the lower damped irradiated lateral phase. The calculated dependences of  $\alpha_{\text{eff}}$  and  $\tau_r$  are shown. The linear dependence of the relaxation time is shown in the inset of (c).

irradiation pattern, a linear change from 0 to 1 of irradiated fraction  $x_{\text{irr}}$  is obtained on a single sample [Fig. 5(b)]. Thereby, sample-to-sample variations are excluded. The dependency of  $\alpha_{\text{eff}}$  and  $\tau_r$  with material fraction after Ni irradiation with a fluence of  $2 \times 10^{14}$  is plotted in Fig. 5(c). In addition, the data are also compared to macrospin simulations of the magnetic response to a pulsed magnetic-field excitation, as in the experiments, by solving the Landau-Lifschitz-Gilbert equation.<sup>33</sup> The calculated results, assuming a superposition of both material fractions and analyzed analog to the experimental data, are added to Fig. 5(c).  $\tau_r$  changes the fraction of the irradiated area linearly with  $x_{\text{irr}}$ . The overall value  $\alpha_{\text{eff}}$  thereby varies with

$$\frac{1}{\alpha_{\text{eff}}^x} = \frac{1}{\alpha_{\text{eff}}^{\text{irr}}} x_{\text{irr}} + \frac{1}{\alpha_{\text{eff}}^{\text{nonirr}}} (1 - x_{\text{irr}}) \quad (2)$$

from the initial damping parameter value  $\alpha_{\text{eff}}^{\text{nonirr}}$  to  $\alpha_{\text{eff}}^{\text{irr}}$  with  $x_{\text{irr}}$ . In accordance with the results presented before (compare to Fig. 4), the precessional frequency increases slightly with  $x_{\text{irr}}$ .

#### IV. CONCLUSION

In conclusion, we demonstrate the use of ultrathin layers of AF materials to laterally manipulate and adjust the effective dynamic magnetic properties of F thin films over a wide

range. The controlled local modification is achieved by ion irradiation, due to ion-induced alterations of coupling across the F-AF interface structure. In the resulting mixed property film, the magnetic damping parameter is a result from a direct superposition of the individual relaxation-time contributions. Elementary dependencies to describe the effect of irradiation fluence and the hybrid magnetic properties are established. Due to the interfacial origin of the effect, the magnetic parameter changes will scale inversely proportional to the ferromagnetic thin-film thickness. Preparing layered F-AF films with mixed multiphase effective properties provides an alternative route for the tailoring of dynamic magnetic properties in soft-magnetic thin films. It should be extendable to other magnetic multilayer samples, exhibiting enhanced interfacial spin scattering.

#### ACKNOWLEDGMENTS

The authors thank K. Kirsch for help with the film deposition, I. Winkler for help with the ion irradiation, and M. Fritzsche for help with TEM investigations. J.M. and J.F. gratefully acknowledge the support of the Deutsche Forschungsgemeinschaft (DFG MC9/7 and FA314/3). A part of the initial research was performed at the IFW Dresden.

\*j.mccord@hzdr.de

- <sup>1</sup>J. A. Katine, F. J. Albert, R. A. Buhrman, E. B. Myers, and D. C. Ralph, *Phys. Rev. Lett.* **84**, 3149 (2000).
- <sup>2</sup>C. Chappert, A. Fert, and F. N. Van Dau, *Nat. Mater.* **6**, 813 (2007).
- <sup>3</sup>S. Parkin, M. Hayashi, and L. Thomas, *Science* **320**, 190 (2008).
- <sup>4</sup>R. O'Handley, *Modern Magnetic Materials: Principles and Applications* (Wiley, New York, 1998).
- <sup>5</sup>S. G. Reidy, L. Cheng, and W. E. Bailey, *Appl. Phys. Lett.* **82**, 1254 (2004).
- <sup>6</sup>A. Rebei and J. Hohlfield, *Phys. Rev. Lett.* **97**, 117601 (2006).
- <sup>7</sup>J. O. Rantschler, R. D. McMichael, A. Castillo, A. J. Shapiro, W. F. Egelhoff, B. B. Maranville, D. Pulugutha, A. P. Chen, and L. M. Connors, *J. Appl. Phys.* **101**, 033911 (2007).
- <sup>8</sup>G. Woltersdorf, M. Kiessling, G. Meyer, J.-U. Thiele, and C. H. Back, *Phys. Rev. Lett.* **102**, 257602 (2009).
- <sup>9</sup>P. F. Carcia, A. D. Meinhaldt, and A. Suna, *Appl. Phys. Lett.* **47**, 178 (1985).
- <sup>10</sup>C. Chappert *et al.*, *Science* **280**, 1919 (1998).
- <sup>11</sup>S. Demokritov, C. Bayer, S. Poppe, M. Rickart, J. Fassbender, B. Hillebrands, D. Kholin, N. Kreines, and O. Liedke, *Phys. Rev. Lett.* **90**, 097201 (2003).
- <sup>12</sup>W. H. Meiklejohn and C. P. Bean, *Phys. Rev.* **102**, 1413 (1956).
- <sup>13</sup>J. Nogues and I. K. Schuller, *J. Magn. Magn. Mater.* **192**, 203 (1999).
- <sup>14</sup>A. Berkowitz and K. Takano, *J. Magn. Magn. Mater.* **200**, 552 (1999).
- <sup>15</sup>F. Radu and H. Zabel, in *Magnetic Heterostructures, Advances and Perspectives in Spinstructures and Spintransport*, edited by H. Zabel and S. D. Bader, Springer Tracts in Modern Physics Vol. 227 (Springer, Berlin, 2008), pp. 97–183.
- <sup>16</sup>R. D. McMichael, M. D. Stiles, P. J. Chen, and W. F. Egelhoff, *J. Appl. Phys.* **83**, 7037 (1998).

- <sup>17</sup>J. McCord, R. Mattheis, and D. Elefant, *Phys. Rev. B* **71**, 094420 (2005).
- <sup>18</sup>J. McCord, R. Kaltofen, T. Gemming, R. Hühne, and L. Schultz, *Phys. Rev. B* **75**, 134418 (2007).
- <sup>19</sup>J. McCord, R. Kaltofen, O. G. Schmidt, and L. Schultz, *Appl. Phys. Lett.* **92**, 162506 (2008).
- <sup>20</sup>B. K. Kuanr, R. E. Camley, and Z. Celinski, *J. Appl. Phys.* **93**, 7723 (2003).
- <sup>21</sup>R. D. McMichael, C. G. Lee, J. E. Bonevich, P. J. Chen, W. Miller, and W. F. Egelhoff, *J. Appl. Phys.* **88**, 5296 (2000).
- <sup>22</sup>M. Ali, C. H. Marrows, M. Al-Jawad, B. J. Hickey, A. Misra, U. Nowak, and K. D. Usadel, *Phys. Rev. B* **68**, 214420 (2003).
- <sup>23</sup>G. Malinowski, M. Hehn, and P. Panissod, *J. Phys. Condens. Matter* **18**, 3385 (2006).
- <sup>24</sup>A. B. Kos, T. J. Silva, and P. Kabos, *Rev. Sci. Instrum.* **73**, 3563 (2002).
- <sup>25</sup>G. Sandler, H. Bertram, T. J. Silva, and T. Crawford, *J. Appl. Phys.* **85**, 5080 (1999).
- <sup>26</sup>J. Ziegler [<http://www.srim.org/>].
- <sup>27</sup>W. Möller and W. Eckstein, *Nucl. Instrum. Methods B* **2**, 814 (1984).
- <sup>28</sup>A. Mougin, T. Mewes, M. Jung, D. Engel, A. Ehresmann, H. Schmoranzer, J. Fassbender, and B. Hillebrands, *Phys. Rev. B* **63**, 060409 (2001).
- <sup>29</sup>S. O. Demokritov, C. Bayer, S. Poppe, M. Rickart, J. Fassbender, B. Hillebrands, D. I. Kholin, N. M. Kreines, and O. M. Liedke, *Phys. Rev. Lett.* **90**, 097201 (2003).
- <sup>30</sup>J. Fassbender and J. McCord, *Appl. Phys. Lett.* **88**, 252501 (2006).
- <sup>31</sup>J. McCord, I. Mönch, J. Fassbender, A. Gerber, and E. Quandt, *J. Phys. D* **42**, 055006 (2009).
- <sup>32</sup>N. J. Gökemeijer, T. Ambrose, and C. L. Chien, *Phys. Rev. Lett.* **79**, 4270 (1997).
- <sup>33</sup>T. Gilbert, *IEEE Trans. Magn.* **40**, 3443 (2004).